Available online at www.sciencedirect.com
ScienceDirect
Journal of Photochemistry and Photobiology A: Chemistry 191 (2007) 176–181
Journal of Photochemistry and Photobiology A:Chemistry
www.elsevier.com/locate/jphotochem

Intramolecular electronic energy transfer in rhodamine–azulene bichromophoric molecule

Olga Kuznetz, Daly Davis, Husein Salman, Yoav Eichen, Shammai Speiser *

Schulich Faculty of Chemistry, Technion-Israel Institute of Technology, Haifa 32000, Israel

Received 12 February 2007; received in revised form 15 April 2007; accepted 24 April 2007
Available online 3 May 2007

Abstract

Electron transfer and electronic energy transfer (EET) processes are ways by which different molecules can interact, signalling their state, by EET from a donor (D) to an acceptor (A). This D–A transfer is often observed in an intermolecular process but it can also occur intramolecularly, that is between two bridged parts of a bichromophoric molecule. In this paper we present results pertaining to electronic energy transfer in a newly synthesized rhodamine–azulene (Rh–Az) a bichromophoric molecule, in which a full adder can be implemented. The intramolecular EET rate constant in the Rh–Az molecule was found to be $7.81 \times 10^9\ s^{-1}$.

Keywords: Rhodamine; Azulene; Electronic energy transfer

1. Introduction

Interaction between excited and ground states of two molecules involving electronic energy transfer (EET) has been the subject of considerable interest [1]. This process plays a key role in chemistry, biology and physics and is well documented and rather well understood. EET can be observed to occur in an intermolecular fashion between separate donor, D, and acceptor, A, molecules or intramolecularly in a bichromophoric molecule where D and A moieties are chemically connected by a molecular bridge, B. The first observation of short range intramolecular EET (Intra-EET) was reported by Schnepp and Levy for the naphthalene-$(CH_2)_n$-anthracene system [2]. Later, many other groups examined other bichromophoric systems [1]. The occurrence of intra-EET could be readily evaluated from the excitation and emission spectra of each moiety alone and comparison with the corresponding spectra of the bichromophoric molecules. The basic intra-EET process can be described by Eq. (1):

$$D* –B–A \xrightarrow{k_{ET}} D–B–A*, \quad (1)$$

Here the excitation energy is transferred from an excited donor D* chromophore to a ground state acceptor moiety A, resulting in quenching of D* fluorescence and excitation of A. B may act as a mere molecular spacer connecting the two chromophores, or it may play a major role in promoting the transfer process [3]. In most cases the Intra-EET rate constant, $k_{ET,}$ is attributed to two possible contributions. The first is the long range Coulombic contribution which was formulated by Förster in terms of dipole–dipole interaction [4]. Using the expressions for absorption coefficient of the acceptor $\varepsilon_A(\lambda)$ and the normalized emission spectral distribution of the donor $F_D(\lambda)$ the Förster expression for dipole–dipole induced EET rate constant may be obtained, as it is shown in Eq. (2):

$$k_{ET}^{d–d} = \frac{Q_D \kappa^2}{\tau_D R^6} \left(\frac{9000(\ln 10)}{128\pi^5 N n^4} \right) \int_0^\infty F_D(\lambda)\varepsilon_A(\lambda)\lambda^4 \, d\lambda \quad (2)$$

where $F_D(\lambda)$ is the normalized fluorescence intensity of the donor, $\varepsilon_A(\lambda)$ the extinction coefficient of the acceptor (in $M^{-1}\,cm^{-1}$), Q_D the fluorescence quantum yield of the donor in the absence of the acceptor, N denotes Avogadro number, n the refractive index of medium, τ_D the lifetime of the donor in the absence of an acceptor and R is the distance between the donor and the acceptor. κ^2 is an orientation factor that can take values from 0 (for perpendicular to transition moments) to 4 (collinear to transition moments). When the transition dipole moments are parallel, $\kappa^2 = 1$. When the molecules are free to rotate at a rate that is much faster than the de-excitation rate of the donor, the

* Corresponding author. Tel.: +972 4 8293735; fax: +972 4 8295703.
E-mail address: speiser@technion.ac.il (S. Speiser).

1010-6030/$ – see front matter © 2007 Elsevier B.V. All rights reserved.
doi:10.1016/j.jphotochem.2007.04.020

averaging value of κ^2 is 2/3 [4]. Equation (2) is often written in terms of the Förster critical transfer radius, R_0:

$$k_{ET}^{d-d} = \frac{1}{\tau_D}\left(\frac{R_0}{R}\right)^6 \quad (3)$$

From Eqs. (2) and (3) we obtain the expression for Förster distance (R_0), Eq. (4):

$$R_0^6 = \frac{9000(\ln 10)\kappa^2 Q_D}{128\pi^5 Nn^4}\int_0^\infty F_D(\lambda)\varepsilon_A(\lambda)\lambda^4\,d\lambda \quad (4)$$

Another contribution to EET is the short range exchange interaction, as formulated by Dexter [5]. The rate of dipole–dipole induced EET decreases as R^{-6} whereas that of the exchange induced process decreases as $\exp(-2R/L)$, R being the interchromophore distance and L being the average van der Waals radius for the overlapping orbitals.

Recently we have we proposed to use EET as a way of connecting between logical operations that are implemented on different molecules. We have discussed [6] the photophysics of a full adder and suggested the azulene–rhodamine 6G molecular system. An essential process for such a full adder scheme is an efficient excitation transfer mechanism to allow concatenation of the two half adder molecular moieties that comprise the full adder. Previous studies in this molecular system centered around processes involving the S_2 electronic states in azulene and rhodamine [7–11]. Since no relevant data on EET between rhodamine S_1 state and azulene S_1 is available we have investigated a specially designed bichromphoric molecule comprised of azulene and rhodamine moieties in which we show the existence of such an efficient EET process.

2. Experimental

The synthesis of these novel molecules, 4-azulene-1-ly-butylamine, **1**, Az-amine, and the bichromophric molecule **2**, Rh–Az, is described elsewhere [12], commercially available spectral grade RhodamineB isothiocyanate was used without further purification. The molecular structures of these compounds are shown in Fig. 1.Standard absorption measurements were made on Shimadzu UV-1601 UV–Vis spectrophotometer and fluorescence and excitation spectra were taken on a Perkin-Elmer LS 50 spectrofluorimeter.

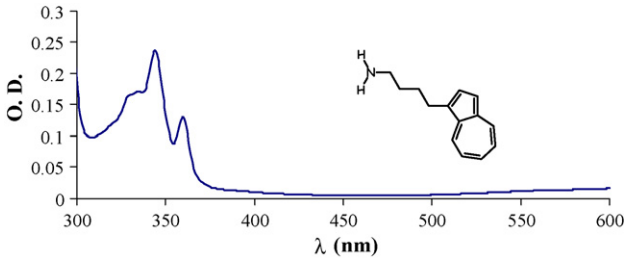

Fig. 2. Absorption spectrum of low concentration Az-amine solution showing the $S_0 \rightarrow S_2$ absorption band at 344 nm.

For most measurements of Rh–Az emission spectroscopy a solution concentration corresponding approximately to OD = 0.2 of the Rh moiety (545 nm peak of the $S_0 \rightarrow S_1$ absorption) was kept. The same was applied for the other molecules such as 4-azulene-1-ly-butylamine (Az-amine) molecule for which concentration corresponding approximately to OD = 0.2 at 344 nm, of the $S_0 \rightarrow S_2$ absorption peak, was kept along most of the measurements. Highly concentrated solutions (OD higher then 2 at the peak mentioned above) were used for the characterization of the weak absorption to the S_1 excited state of the azulene moiety in Rh–Az and of Az-amine.

3. Results and discussion

3.1. Spectroscopy of the Rh–Az molecular system

Absorption, emission and excitation spectra were measured at room temperature, in methanol solutions. Our first goal was to establish all transition energies associated with the rhodamine and azulene moieties of the novel Rh–Az bichromophoric molecule.

The absorption spectra of **1** at low and high concentrations are shown in Figs. 2 and 3, respectively. The $S_0 \rightarrow S_1$ and the $S_0 \rightarrow S_2$ peak absorption bands of **1** are at 601 and 344 nm, respectively.

Excitation of **1** at 344 nm results in dual fluorescence from S_2 (385 nm peak) and from S_1 (730–770 nm wide peak) excited levels. The $S_1 \rightarrow S_0$ emission intensity is weak compared to that from the S_2 level. Excitation spectrum of the molecule at 384 nm produces a mirror image of the emission spectrum with the 345 nm peak position, which is exactly the same peak position of $S_0 \rightarrow S_2$ absorption band (Fig. 4). These spectra are typical

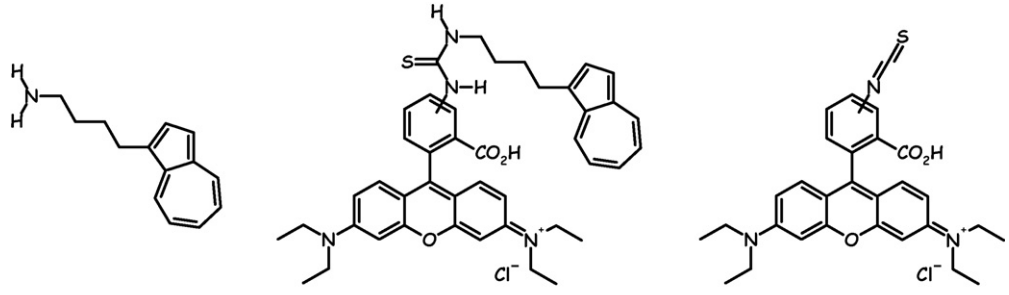

Fig. 1. Molecular structures of the novel bichromophoric molecule **2**, Rh–Az together with the single chromophores **1**, Az-amine and **3**, RhodamineB isocyanate.

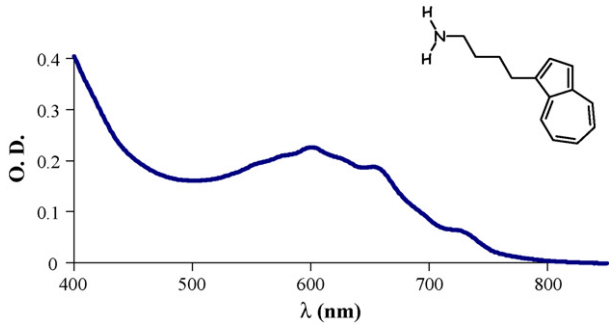

Fig. 3. Absorption spectrum of highly concentrated Az-amine solution showing the $S_0 \rightarrow S_1$ absorption band at 601 nm.

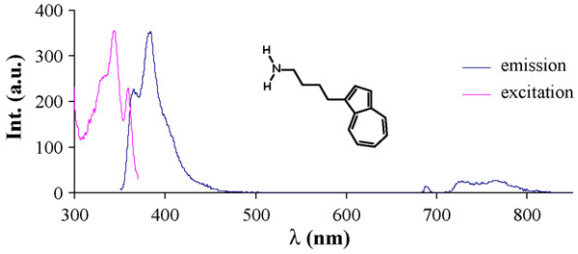

Fig. 4. Emission and excitation spectra of **1**, $\lambda_{ex} = 344$ nm and $\lambda_{em} = 384$ nm.

of azulene and other azulene derivatives. This molecule serves as the reference azulene chromophore for the Rh–Az system.

The absorption, fluorescence and excitation spectra of **3** are shown in Figs. 5 and 6 respectively showing the $S_0 \rightarrow S_1$ absorption band of the RhB isocyanate at 543 nm and the $S_1 \rightarrow S_0$ fluorescence band of the molecule at 574 nm. This molecule serves as the reference rhodamine chromophore for the Rh–Az.

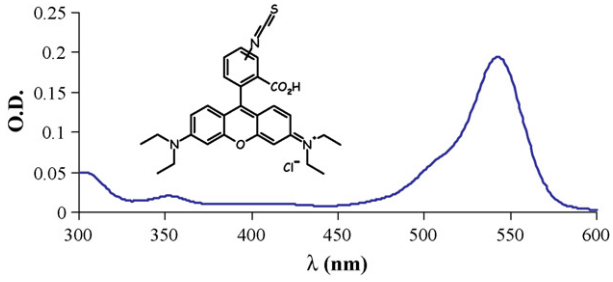

Fig. 5. Absorption spectrum of 2.86×10^{-6} M methanol solution of **3**.

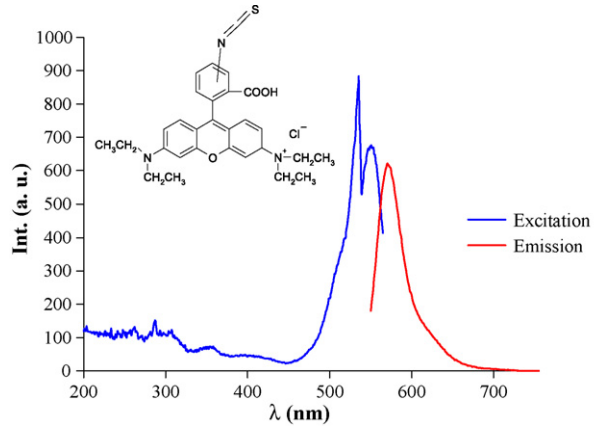

Fig. 6. Emission and excitation spectra of 2.86×10^{-6} M methanol solution of **3**, $\lambda_{ex} = 543$ nm and $\lambda_{em} = 572$ nm.

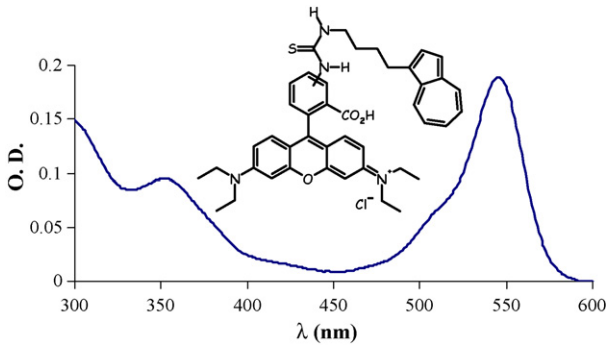

Fig. 7. Absorption spectrum of low concentration Rh–Az solution.

Absorption spectra of Rh–Az at low and high concentrations are shown at Figs. 7 and 8, respectively. It is evident from Fig. 7 that the $S_0 \rightarrow S_1$ absorption band of the rhodamine moiety is at 545 nm and the $S_0 \rightarrow S_2$ absorption band of the azulene chromophore is at 350 nm, with some contribution from overlap with the $S_0 \rightarrow S_2$ absorption band of the rhodamine moiety. Fig. 8 shows the $S_0 \rightarrow S_1$ weak absorption of the azulene moiety at 645 nm, as a shoulder on the long tail $S_0 \rightarrow S_1$ absorption band of the rhodamine moiety. These spectra indicate that Rh–Az is a bichromophoric molecule for which the absorption spectrum of the molecule is a superposition of the absorption spectra of its two chromophores **3** and **1** (Figs. 2, 3 and 5).

Fig. 9 shows the emission and excitation spectra of Rh–Az, where the excitation is at the $S_0 \rightarrow S_1$ transition of the rhodamine

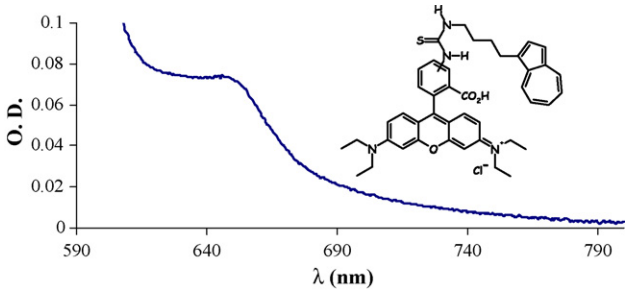

Fig. 8. Absorption spectrum of Rh–Az (highly concentrated solution).

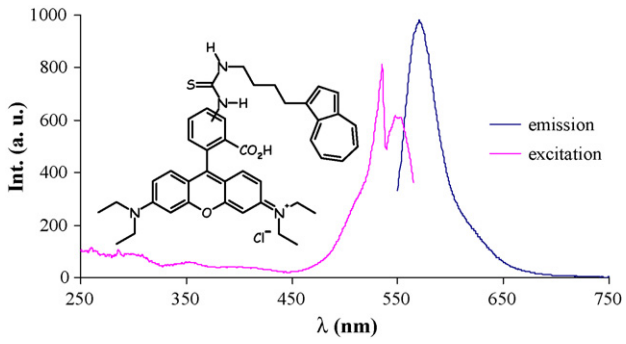

Fig. 9. Emission and excitation spectra of Rh–Az, $\lambda_{ex} = 545$ nm and $\lambda_{em} = 570$ nm.

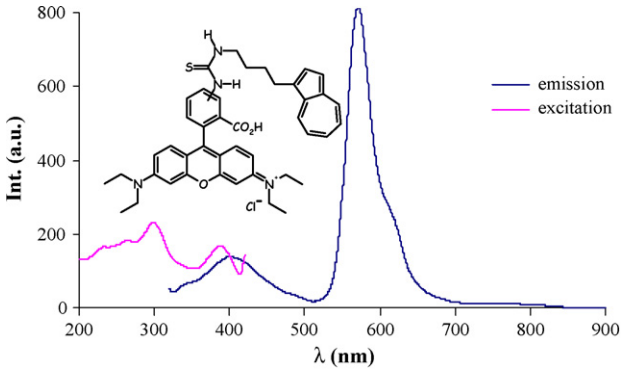

Fig. 10. Emission and excitation spectra of Rh–Az, $\lambda_{ex} = 310$ nm and $\lambda_{em} = 440$ nm.

moiety. It can be seen that the $S_1 \rightarrow S_0$ fluorescence band of the rhodamie moiety of Rh–Az is at 572 nm. Almost the same emission and excitation spectra ($\lambda_{ex} = 545$ nm, $\lambda_{em} = 572$ nm) were obtained for the reference molecule **3** (Fig. 6).

The sharp feature around 530 nm might be attributed to an isomer form of the molecule.

Upon excitation of S_2 state of the azulene moiety at 310 nm the dual fluorescence spectrum, shown in Fig. 10 is observed. The $S_2 \rightarrow S_0$ fluorescence band of the azulene moiety is seen at 405 nm and the $S_1 \rightarrow S_0$ emission band of rhodamine is at 570 nm. It can be seen, that the fluorescence from the S_2 excited state of the azulene moiety is highly quenched due to an efficient intramolecular EET process to the rhodamine moiety. It is similar in nature to that observed for the corresponding intermolecular EET in the azulene–rhodanine6G system [9].The excitation spectrum of the molecule shows two peaks at 300 and 395 nm. Comparing to the absorption spectrum (Fig. 7), one can see that these peaks correspond to the overlapping $S_0 \rightarrow S_2$ absorption of the rhodamine and azulene moieties which can only be resolved in the excitation spectrum, where the azulene spectrum is enhanced due to its much higher $S_2 \rightarrow S_0$ fluorescence quantum yield.

3.2. Intermolecular energy transfer in the Rh6G–Az system

Although rhodamine6G and azulene is a well-known donor–acceptor pair system, there are no reports of measuring the critical transfer radius for the EET process from an excited rhodamine to the S_1 state of azulene. In order to calculate the critical transfer radius the $S_0 \rightarrow S_1$ azulene absorption spectrum and the $S_1 \rightarrow S_0$ rhodamine6G emission spectrum were measured. These overlapping spectra are shown at Fig. 11. The solutions concentrations were 4×10^{-4} and 1×10^{-6} M for Az and rhodamine6G, respectively. Examination of Fig. 11 shows good overlap between $S_0 \rightarrow S_1$ Az absorption and the $S_1 \rightarrow S_0$ emission spectrum of rhodamine6G. From these spectra we can calculate the spectral overlap integral given by

$$J(\lambda) = \int_0^\infty F_D(\lambda)\varepsilon_A(\lambda)\lambda^4 \, d\lambda \quad (5)$$

Utilizing Eq. (4) and the calculated value of the overlap integral we can obtain the Förster critical transfer radius for the

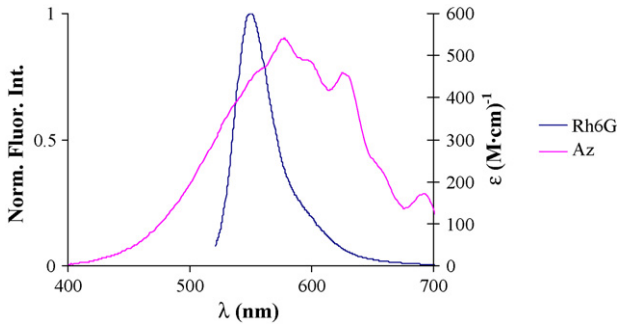

Fig. 11. Spectral overlap between azulene absorption and rhodamine6G $S_1 \rightarrow S_0$ fluorescence spectra.

rhodamine6G and azulene donor–acceptor couple. Where the refractive index of the medium (methanol) is 1.331, the fluorescence quantum yield for rhodamine6G is 0.94 [11] and κ^2 is 2/3. The calculations yield the R_0 value of 96.60 Å for this couple. Such an R_0 value is suitable for an efficient long-range EET via dipole–dipole interaction. In order to measure the critical transfer radius we have also followed quenching of rhodamine6G fluorescence by azulene. The corresponding Stern–Volmer plot for rhodamine6G-donor $S_1 \rightarrow S_0$ fluorescence quenching by azulene-acceptor is shown in Fig. 12 where the fluorescence intensity was corrected for donor solution dilution.

The donor's quenching follows the simple Stern–Volmer quenching relation (Eq. (6)):

$$\frac{I_0}{I} = 1 + k_q \tau_0 [Q] \quad (6)$$

where I_0 is the steady state fluorescence intensity in the absence of quencher, I the steady state fluorescence intensity in the presence of quencher at concentration $[Q]$, τ_0 the donor's lifetime in the absence of quencher and k_q is the bimolecular quenching rate constant.

Utilizing Eq. (6) we have calculated the bimolecular quenching constant, k_q to be 5.44×10^{11} L mol^{-1} s^{-1}), using $\tau_0 = 4.13$ ns value for rhodamine6G dissolved in methanol [11]. The corresponding bimolecular quenching rate constant for a diffusion limited quenching process was calculated, using the viscosity for methanol at 300 K to be 1.22×10^{10} L mol^{-1} s^{-1}) [1]. Comparing these two bimolecular quenching constant values we see that Stern–Volmer quenching constant is approximately 45 times higher than diffusion limited one, indicating

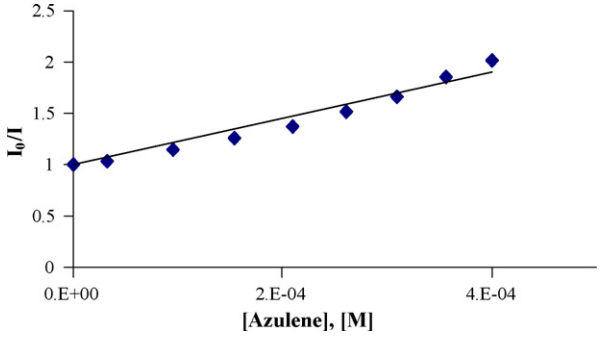

Fig. 12. Stern–Volmer plot for the rhodamine6G–azulene molecular system.

that the quenching mechanism is energy transfer between rhodamine6G and azulene.

The Stern–Volmer experiment enables also to calculate the Förster distance between the donor and the acceptor. The expression for the critical transfer radius (in Å) is given by Eq. (7) [4,11]:

$$R_0 = \frac{7.35}{[Q]_{1/2}^{1/3}} \tag{7}$$

where $[Q]_{1/2}$ is the quencher molar concentration for which $I_0/I = 2$. From Fig. 12 we obtain that the azulene concentration needed for 50% quenching of rhodamine fluorescence is 4.45×10^{-4} M. Using Eq. (7), the Förster critical transfer radius between rhodamine6G and azulene was calculated. The value obtained is 96.25 Å in a very good agreement with the theoretical value. This study shows that the main contribution to EET in this couple is the dipole-dipole long-range mechanism and contribution from Dexter exchange interaction is not significant.

3.3. Intramolecular energy transfer in the Rh–Az system

Fig. 13 shows the fluorescence of the S_1 state of the azulene moiety of the Rh–Az molecule, excited at 645 nm (see Fig. 8). The very weak $S_1 \rightarrow S_0$ fluorescence of azulene, peaking at 780 nm is observed at the tail of the rhodamine fluorescence, peaking at 570 nm (see Fig. 9), is observed. The excitation spectrum of the molecule monitored at the azulene $S_1 \rightarrow S_0$ fluorescence peak of 780 nm matches the absorption spectrum of Rh–Az (Fig. 7), showing both the $S_0 \rightarrow S_1$ band of the rhodamine moiety is at 533 nm and, and the $S_0 \rightarrow S_2$ absorption band of the azulene moiety at 380 nm. The assignment of the various peaks was done by comparison with the corresponding spectra of the individual moieties Figs. 2–6. By comparing the absorption (Fig. 7) and excitation spectra of Rh–Az, we see that the $S_0 \rightarrow S_2$ peak intensity of the azulene moiety in the absorption spectrum is lower than that observed in the excitation spectrum. The opposite behavior is observed for the $S_0 \rightarrow S_1$ band of the rhodamine moiety. Here the $S_0 \rightarrow S_1$ peak intensity absorption spectrum is higher than the corresponding one in the excitation spectrum. This change in peaks intensity ratio together with appearance of the $S_1 \rightarrow S_0$ fluorescence for azulene upon excitation of the rhodamine moiety at 645 nm, are clear

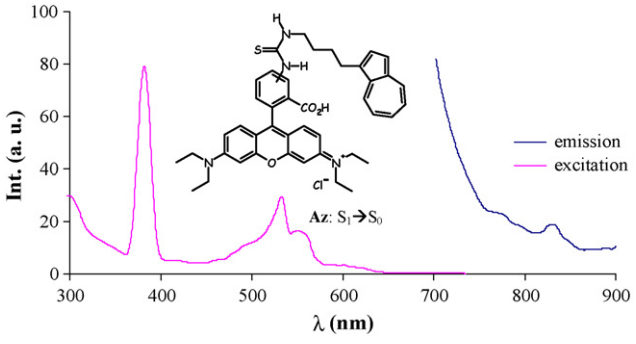

Fig. 13. Emission and excitation spectra of Rh–Az (high concentration), $\lambda_{ex} = 645$ nm and $\lambda_{em} = 765$ nm.

evidence for intramolecular electronic energy transfer from the rhodamine moiety to the azulene chromophore in Rh–Az. From these and utilizing Eq. (8), we can calculate the intra-EET yield:

$$\frac{I_{Az(Rh-Az)}}{I_{Rh(Rh-Az)}} = \frac{\varepsilon_{Az}}{\varepsilon_{Rh}} \frac{\Phi_{Az}^{S_2 \rightarrow S_0}}{\Phi_{Rh(Rh-Az)}} \tag{8}$$

where $I_{Az(Rh-Az)}$ is the azulene moiety $S_0 \rightarrow S_2$ transition intensity in the excitation spectrum(Fig. 12), $I_{Rh(Rh-Az)}$ the rhodamine moiety $S_0 \rightarrow S_1$ transition intensity in the excitation spectrum(Fig. 12), ε_{Az} the azulene moiety molar extinction coefficient of the $S_0 \rightarrow S_2$ transition (Fig. 9), ε_{Rh} the rhodamine molar extinction coefficient of the $S_0 \rightarrow S_1$ transition (Fig. 9), $\Phi_{Az}^{S_2 \rightarrow S_0}$ is the azulene $S_2 \rightarrow S_0$ emission quantum yield ($\Phi_{Az}^{S_2 \rightarrow S_0} = 0.24$) and $\Phi_{Rh(Rh-Az)}$ is the rhodamine moiety $S_1 \rightarrow S_0$ emission quantum yield.

Substituting all the values into Eq. (8) yields that $\Phi_{Rh(Rh-Az)} = 0.04$. This means that 96% of EET was transferred from Rh moiety to Az, i.e. the intra-EET quantum yield is $\Phi_{ET} = 0.96$.

From the relation:

$$\Phi_{ET} = \frac{k_{ET}}{k_{ET} + 1/\tau_f} \tag{9}$$

we can estimate the intra-EET rate constant (k_{ET}) from the rhodamine moiety to the azulene chromophore. Where in Eq. (9) τ_f is the $S_1 \rightarrow S_0$ emission lifetime of rhodamineB ($\tau_f = 3.2$ ns). Thus we obtain for Rh–Az that $k_{ET} = 7.81 \times 10^9$ s^{-1}.

In order to determine the spatial orientation of the rhodamine and azulene chromophores within Rh–Az a calculation of the optimized molecular geometry were performed. The ground state geometry of the molecule was optimized at the restricted Hartree–Fock level using a Slater type orbital Gaussian basis (STO-3G). All the structure optimization and calculations were performed using GAMESS program.

The optimized structure of Rh–Az is shown in Fig. 14. The geometry optimization together with the excited state energies of the molecule enables us to estimate the following parameters: R is the distance between donor (rhodamine) and acceptor (azulene) moieties, the donor and acceptor transition dipoles vectors (M_D and M_A, respectively), the angles between the donor and acceptor axes: θ_A, θ_D and θ_{DA}. Using Eq. (10), we can easily obtain the κ^2 value [1]. The results are shown in Table 1:

$$\kappa^2 = \cos\theta_{DA} - 3\cos\theta_D \cos\theta_A = \sin\theta_D \sin\theta_A \cos\varphi - 2\cos\theta_D \cos\theta_A \tag{10}$$

Table 1
Energy transfer geometrical parameters for Rh–Az

Parameter	Value
R (Å)	9.6
M_A (Debye)	2.21
M_D (Debye)	0.30
θ_A (°)	76.58
θ_D (°)	90.23
θ_{DA} (°)	87.89
κ^2	0.04

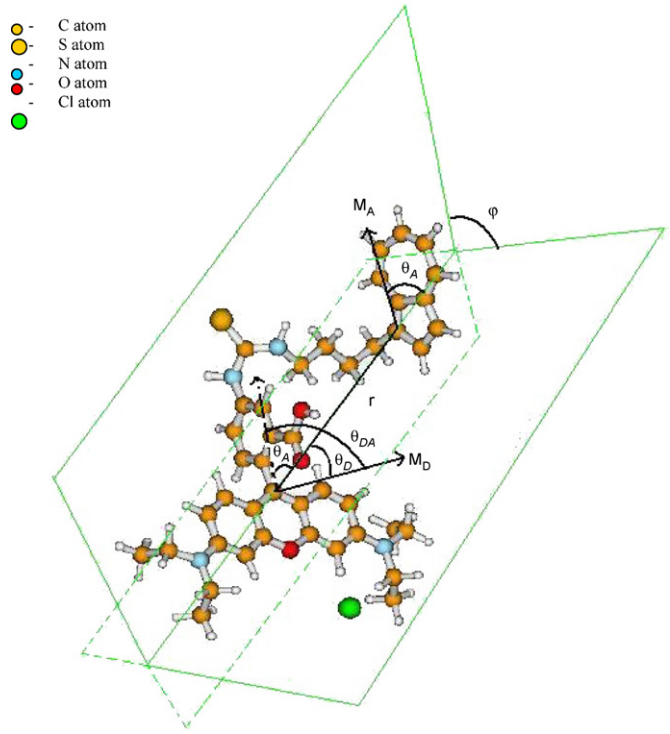

Fig. 14. Optimized calculated structure of Rh–Az.

Using Eq. (2) the dipole–dipole induced EET rate constant (k_{ET}) for randomly orientated rhodamine and azulene moieties can be obtained. The parameters substituted into the equation were: $R = 9.6$ Å, $R_0 = 96.69$ Å, $\tau_D = 3.2 \times 10^{-9}\ s^{-1}$ yielding k_{ET} was $3.26 \times 10^{14}\ s^{-1}$. This value is much higher than the experimental one indicating that in Rh–Az the two moieties are not randomly orientated thus reducing k_{ET}. By substituting the experimental value for k_{ET} into Eq. (10) we obtain the experimental value of orientation factor κ^2, as 0.11. This is in reasonable agreement to the calculated value of 0.04 given in Table 1.The discrepancy can be attributed to the shortcomings of the calculation procedure as well as to the fact that at 9.6 Å distance between the two chromophores Forster theory, valid for point dipole can only give approximate results.

4. Conclusions

In this paper we have presented results pertaining to the intramolecular electronic transfer process between the S_1 of rhodamine and azulene moieties in Rh–Az, a novel bichromophoric molecular system. In addition we have investigated the spectroscopy of a new derivative of azulene. We have found that the Intra-EET rate for Rh–Az is $7.81 \times 10^9\ s^{-1}$, suitable to communicate logic information between the moieties essential for implementation of a full logic adder on a single molecule [12,13].

Acknowledgments

This research was supported by the Fund for the Promotion of Research at the Technion and the Technion VPR Fund.

References

[1] S. Speiser, Chem. Rev. 96 (1996) 1953.
[2] O. Schnepp, M. Levy, J. Am. Chem. Soc. 84 (1962) 172.
[3] N. Lokan, M.N. Paddow-Row, T.A. Smith, M. LaRosa, K.P. Ghiggino, S. Speiser, J. Am. Chem. Soc. 121 (1999) 2917.
[4] Th. Förster, in: O. Sinanoglu (Ed.), Modern Quantum Chemistry, vol. 3, Academic Press, New York, 1968, p. 93.
[5] D.L. Dexter, J. Chem. Phys. 2 (1953) 836.
[6] F. Remacle, S. Speiser, R.D. Levine, J. Phys. Chem. A 105 (2001) 5589.
[7] I. Kaplan, J. Jortner, J. Chem. Phys. Lett. 52 (1977) 202.
[8] I. Kaplan, J. Jortner, Chem. Phys. 32 (1978) 381.
[9] S. Speiser, Appl. Phys. B 49 (1989) 109.
[10] M. Orenstein, S. Kimel, S. Speiser, Chem. Phys. Lett. 58 (1978) 582.
[11] S. Speiser, N. Shakkour, Appl. Phys. B 38 (1985) 191.
[12] H. Salman, Y. Eichen, S. Speiser, Mater. Sci. Eng. C 26 (2006) 881.
[13] O. Kuznetz, H. Salman, Y. Eichen, S. Speiser, All optical half adder and full adder logic circuits based on the rhodamine–azulene molecular system, in preparation.